Effects of Thermal Annealing on the Solvent Additive P3HT $PC_{61}BM$ Bulk Heterojunction Solar Cells *

FAN Xing(樊星)[1,2], ZHAO Su-Ling(赵谡玲)[1,2**], CHEN Yu(陈雨)[3], ZHANG Jie(张杰)[3], YANG Qian-Qian(杨倩倩)[1,2], GONG Wei(龚伟)[1,2], XU Zheng(徐征)[1,2], XU Xu-Rong(徐叙瑢)[1,2]

[1]*Key Laboratory of Luminescence and Optical Information (Ministry of Education), Beijing Jiaotong University, Beijing 100044*

[2]*Institute of Optoelectronics Technology, Beijing Jiaotong University, Beijing 100044*

[3]*Institute of High Energy Physics, Chinese Academy of Sciences, Beijing 100049*

(Received 5 January 2015)

Effects of thermal annealing on the optical, electrical and structural properties of 3 vol% 1,8-diiodoctane added P3HT:$PC_{61}BM$ active layers are investigated, concerning the performance of the bulk heterojunction polymer solar cells by changing the heat temperature. The structure information of the active layer is analyzed by using the grazing incidence wide angle scattering diffraction combined with the optical microscope, light absorption, photoluminescence and the external quantum efficiency spectra. The relationship between the detail of morphology and the optical, electrical properties is investigated.

PACS: 84.60.Jt, 88.40.jr, 79.60.Jv, 68.55.−a DOI: 10.1088/0256-307X/32/5/058401

Organic solar cells (OSCs) have shown great potential providing appealing alternatives for inorganic-based devices.[1−4] OSCs based on the bulk-heterojunction structure composed of regioregular poly(3-hexylthiophene) (P3HT) mixed with [6-6-]-phenylC61butyric acid methyl ester ($PC_{61}BM$) have been extensively investigated due to their self-organized and ordered nano-morphologies with bi-continuous interpenetrated networks of the donor and the acceptor, which result in good optical and electrical properties.[5−10] Effective electron and hole transporting between adjacent ordered crystalline regions is beneficial for percolation routes leading to the bottom and top electrodes due to the good relative alignment.[11,12] Furthermore, in P3HT self-organized lamellar nanoscale crystalline regions, the hole charge mobility is greatest in the backbone direction, lower in the π-stacking direction (conduction by hopping) and negligible in the alkyl direction.[13] To enhance the performance of OSC devices, there are many methods including thermal annealing,[5,14−17] solvent annealing,[17−19] and the use of processing additives.[20−24] Almost all of these treatments to improve the power conversion efficiency (PCE) of OSC are explained as that the morphology of the active layer was improved after treatments. However, the real mechanism of these treatments on the active layer is unclear.

In this Letter, the well-ordered morphology evolution of the P3HT:$PC_{61}BM$ active layers combined with the thermal annealing and processing additive is analyzed according to the measurement of grazing incidence wide angle scattering (GI-WAXS), optical microscopy, absorption, photoluminescence (PL) and the external quantum efficiency (EQE) spectra. The results show that thermal annealing controls the crystallization time of chain stacking of P3HT molecules accompanied by the diffusion and aggregation of $PC_{61}BM$ molecules.

P3HT and $PC_{61}BM$ were dissolved in chlorobenzene, respectively, with the concentration of 30 mg/mL. The mixed solution of P3HT and $PC_{61}BM$ was prepared with the ratio of 1:1. The solution of the blend was homogenized for 8 h. Then a 40-nm layer of PEDOT:PSS was spun on top of the clean ITO layer after 8 min of UV-ozone treatment. After we heated the PEDOT:PSS at 120℃ for 10 min, films of P3HT:$PC_{61}BM$ BHJs were spin-coated at room temperature using the mixed solution with the addition of 3 vol% 1,8-diiodoctane(DIO) as a solvent additive. The spin-coating rate of P3HT:$PC_{61}BM$ BHJ films is 2000 rpm for 60 s. To analyze the effects of the annealing process of the blend films, after the spin-coating, thermal annealing was carried out on a hot plate for 10 min in an environment of N_2. We treated a group of as-spun blend films without or with different temperatures (50℃, 70℃, 90℃, 110℃, 130℃, 150℃). The cathode was formed by depositing thermally 1 nm of LiF then 100 nm of Al under a vacuum ($<2\times10^{-4}$ Pa) on the top of the photoactive layer. The device structure was ITO/PEDOT:PSS/P3HT:$PC_{61}BM$/LiF/Al. The deposited Al electrode area defining the active area of the device is 0.09 cm^2. The current density-voltage (J–V) characteristics were measured with a programmable Keithley 4200 source meter. Power conversion efficiency was calculated from the J–V

*Supported by the National Natural Science Foundation of China under Grant Nos 51272022 and 11474018, the Research Fund for the Doctoral Program of Higher Education of China under Grant No 20120009130005, and the Fundamental Research Funds for the Central Universities under Grant No 2012JBZ001.

**Corresponding author. Email: slzhao@bjtu.edu.cn

characteristics under a solar simulated light irradiation (AM1.5) of 100 mW/cm^2. All the measurements were performed at room temperature in air without any device encapsulation.

The performance of all prepared cells is shown in Fig. 1 and Table 1. The device annealed at 70℃ shows the highest PCE among all devices compared with the as-spun device. The corresponding parameters are as follows: J_{sc} is 7.98 mA/cm^2, V_{oc} is 0.56 V, FF is 67.63%, and η_{eff} is 3.03%.

Table 1. Device parameters.

	J_{sc} (mA/cm^2)	V_{oc} (V)	FF(%)	E_{ff}(%)
25℃/DIO 3%	6.93	0.50	60.31	2.09
50℃/DIO 3%	7.41	0.53	64.07	2.52
70℃/DIO 3%	7.98	0.56	67.63	3.03
90℃/DIO 3%	7.68	0.58	67.39	3.00
110℃/DIO 3%	6.89	0.58	63.06	2.52
130℃/DIO 3%	6.40	0.59	65.55	2.47
150℃/DIO 3%	5.84	0.59	65.52	2.25

It is obvious that V_{oc} of the device increases along with the annealing temperature. It is reported that the HOMO level of P3HT shifts upward and V_{oc} decreases as the P3HT crystallinity increases, due to the fact that higher crystalline P3HT films have a reduced bandgap compared with a film of the lower crystallinity.[17,25,26] The increasing V_{oc} due to annealing mainly results from the interplanar spacing of P3HT molecules rather than the polymer crystalline distribution and the polymer packing order in the molecule domain. To prove it, the structure properties of blend films annealed at different temperatures were investigated by GI-WAXS with photon energy of 8 keV and an incident angle of 0.2°.

The GI-WAXS diffraction intensity pattern contains spot-like or arc-like distribution depending on the spread of the crystallite orientation distribution (shown in Fig. 2(a)). This suggests that the textured films are predominantly in a paracrystalline order with a preferred out-of-plane orientation while in an isotropic inplane[27–29]. We also analyzed the distribution of the (100) scattered intensity as a function of the azimuthal angle χ of the detector (shown in Fig. 2(e)). It is observed that all the blend films have a similar crystalline degree due to their similar integrated intensity of the diffraction spot. To better understand the structural evolution, the out-of-plane (OOP) GIXRDs of different blend films have been detected (shown in Fig. 2(f)). According to the model proposed by Kayunkid *et al.*,[30] the diffraction peak near $2\theta = 5.2°$ corresponds to the crystal face of (100) of P3HT. A strong (h00) series of 3 order diffraction peaks at (100), (200) and (300) due to the P3HT lamellar stacking suggest that the polymer chains are primarily oriented with the thiophene ring edge-on to the substrate. The coherence length (Scherrer's equation $L_c = 2\pi K/\text{FWHM}$, where $K = 0.8$–1)[31] and the interplanar spacing (the Bragg equation $2d\sin\theta = n\lambda$, where $\lambda = 0.1546$ nm) of the P3HT lamellar were calculated according to the diffraction peak position, diffraction peak intensity, and the full width at half maximum (FWHM) provided by the peak of (100) in Fig. 2(f). The calculated results are shown in Fig. 2(g). When the blend films are annealed, the (100) diffraction peak of P3HT shifts to smaller 2θ accompanied by a smaller FWHM. It is obvious that thermal annealing causes the longer coherence length and broader interplanar spacing of P3HT molecules. It was reported that the as-spun blend of P3HT and $PC_{61}BM$ films is a ternary system made of amorphous P3HT, crystalline P3HT, and $PC_{61}BM$ aggregates.[32] Therefore, the increasing (h00) diffraction intensity along with the annealing temperature indicates the formation of larger crystalline regions of P3HT and the diffusion of $PC_{61}BM$ molecules out of the P3HT chains. A longer coherence length due to the well-defined and packed P3HT molecules will yield more efficient carrier transport due to the small resistance in the well-defined and packed P3HT molecules. Therefore, after thermal annealing, the efficient carrier transport occurs in the ordered regions of the BHJ blend film, which is favorable to the efficiency of BHJ solar cells. However, the broader interplanar spacing may result in the weaker interaction between P3HT molecules and influences the carrier transporting.

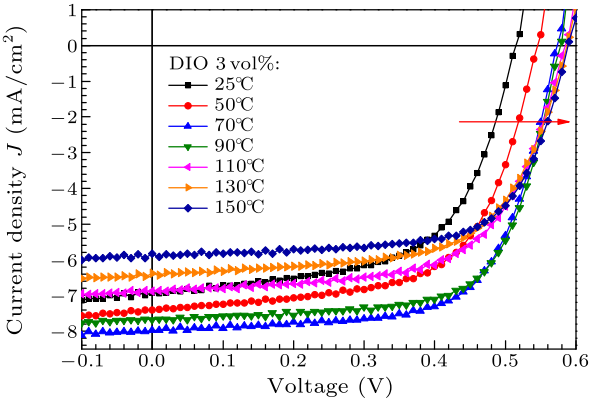

Fig. 1. The current density-voltage (J–V) curves of P3HT:$PC_{61}BM$ BHJ solar cells annealed at different temperatures with 3 vol% DIO added under AM1.5 conditions (100 mW/cm^2).

In as-spun devices, the host solvent CB evaporates much faster than the solvent additive DIO during the drying process due to the lower boiling point of CB. The higher ratio of solvent additive (more amount of DIO) provides a strong driving force for the polymer self-organization and phase separation between P3HT and $PC_{61}BM$ since P3HT is not solvable in DIO solvent while $PC_{61}BM$ is.[33] Therefore, P3HT molecules aggregate with a large average domain size and then the strong interchain-interlayer interaction suppresses the growth of $PC_{61}BM$ aggregation due to the good crystallization of P3HT. The $PC_{61}BM$ aggregation was monitored by the optical microscope

(OM) as shown in Fig. 3. With DIO added, P3HT is driven to self-assemble crystalline domains much faster than $PC_{61}BM$, which allows $PC_{61}BM$ to diffuse into large aggregation. When the blend films were treated under low temperature, the $PC_{61}BM$ aggregation is not uniformly distributed, even though it has a relatively large scale. When the treatment temperature increases, the scale of $PC_{61}BM$ aggregation tends to be smaller firstly due to the faster solvent evaporation then tends to be larger and uniformly distributed. After thermal annealing at 70℃ or 90℃ for 10 min, P3HT:$PC_{61}BM$ blend films have the least amount of $PC_{61}BM$ agglomeration on the mesoscopic scale as shown in Figs. 3(c) and 3(d) compared with other films. It is found that both the blend film without annealing and the blend film under 130℃ annealing show a high phase separation with the large agglomeration of $PC_{61}BM$ as shown in Figs. 3(a) and 3(e), respectively. However, the form of the $PC_{61}BM$ aggregation is different. It is suggested that thermal annealing alters the driving force by changing the time scale which is responsible for the $PC_{61}BM$ domains formation in P3HT:$PC_{61}BM$ blend films. The $PC_{61}BM$ aggregating tendency shows great accordance with J_{sc} and the EQE results we discussed in the following.

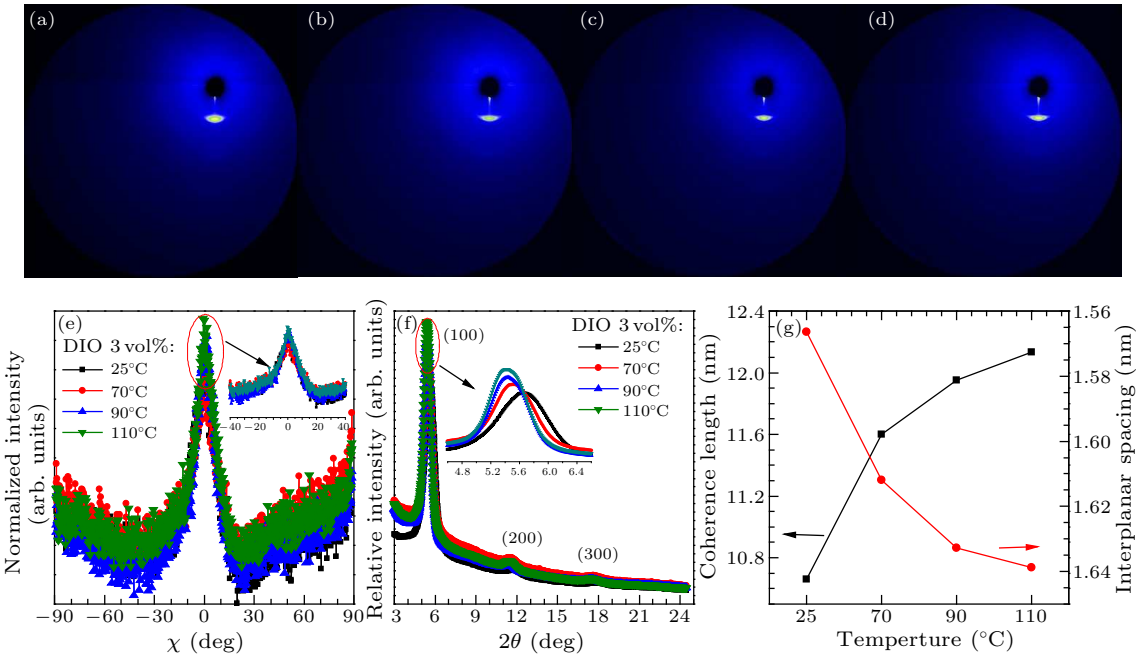

Fig. 2. (a)–(d) GI-WAXS patterns of P3HT:$PC_{61}BM$ blend films annealed at different temperatures (25℃, 70℃, 90℃, 110℃) with 3 vol% DIO added, (e) the integrated tangential line profiles around the spot for the (100) diffraction peak, (f) the out of plane (OOP) line profiles, (g) the coherence length calculated by the Scherrer equation and the interplanar spacing $d(100)$ calculated by the Bragg equation.

As is expected, thermal annealing of 3 vol% DIO added blend films not only influences the morphology but also the optical properties such as the quantity of light absorption and the photoluminescence, as shown in Fig. 4. The blend annealed at 70℃ possesses the highest absorption intensity among these blends. The position of the main absorption peak near 520 nm corresponds to a π–$\pi*$ transition, and the two vibronic 'shoulders' at 550 nm and 600 nm indicate the strong interchain interaction within a high degree of order in P3HT similarly.[34] In addition, the increase of the absorption at 600 nm is assigned to better or larger polymer intraplane stacking, which complements the interplane stacking we mentioned above. The increased absorption has a great influence on the improvement of J_{sc}.[35]

We used photoluminescence measurements to characterize the intimately mixed polymer/fullerene domains in different blend films. All blend films were excited at 520 nm. The emission at 725 nm of blend films originates from the emission of P3HT according to the PL of pure P3HT. All the PL intensity is normalized by the absorption intensity at 520 nm to eliminate the effect of the different absorption intensities of different blend films as shown in Fig. 4(b). The 725 nm intensity of P3HT increases at the annealing temperature 70℃. This suggests that the conjugation length or domain size of P3HT increases[36,37] and the interface area between P3HT and $PC_{61}BM$ decreases.[33] Assuming that the addition of $PC_{61}BM$ only introduces a new exciton quenching pathway, and does not change the properties of the polymer excitons, the PL quenching data can be employed to estimate the upper limit of the diffusion length of a polymer exciton before it reaches the interface of polymer and fullerene domains,[38]

$$L = L_{ex}(1 - \mathrm{PLQ})^{1/2}, \tag{1}$$

where L is the polymer exciton diffusion length, L_{ex} is the exciton diffusion length of the pure polymer (for pure P3HT it is about 10 nm), and PLQ is the fractional PL quenching relative to the pure polymer films and calculated as the ratio of the difference of the integration PL area between blend films and pure polymer to the PL integration area of the pure polymer

$$\mathrm{PLQ} = (\mathrm{PL}_0 - \mathrm{PL})/\mathrm{PL}_0, \qquad (2)$$

where PL and PL_0 are the emission intensities of blend films and pure P3HT. The blend film annealed at 70℃ exhibits the PLQ of 86%. Then the exciton diffusion length L is calculated to be 3.7 nm. The longest exciton diffusion length of the blend film annealed at 70℃ indicates that there are relatively better ordered, purer crystalline polymer domains.[38] This indicates that more effective exciton dissociation and charge transportation occur at the interface.[39,40] The result is consistent with the above-mentioned GI-WAXS results.

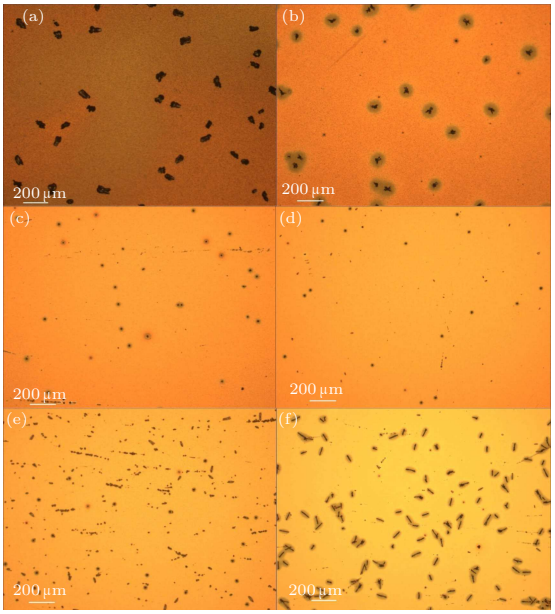

Fig. 3. Microscope images of P3HT:PC61BM blend films annealed at different temperatures (a) 25℃, (b) 50℃, (c) 70℃, (d) 90℃, (e) 110℃ and (f) 130℃ with 3 vol% DIO added.

The external quantum efficiency spectra consisting of the UV-visible absorption spectra of the blend films also confirm the increasing efficiency after annealing shown in Fig. 4(c). It is indicated that the increasing J_{sc} is mainly due to larger P3HT crystalline domains with better packing order and reduced $\mathrm{PC_{61}BM}$ aggregation scale. The efficiencies, especially J_{sc} and FF, show a reduction in devices annealed at temperatures higher than 70℃. The decreasing EQE at 350 nm attributed by $\mathrm{PC_{61}BM}$ suggests the enlarged growth of $\mathrm{PC_{61}BM}$ aggregation at higher temperature,[38] which may result in increasing series resistance and an imbalance of charge transport caused by electrical traps on the charge transport way.

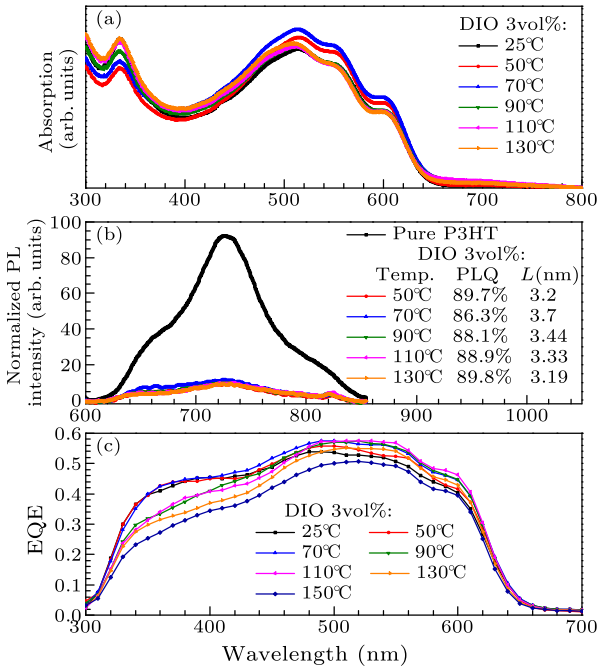

Fig. 4. The UV-visible absorption spectrum (a) and the photoluminescence spectrum (b) of P3HT:$\mathrm{PC_{61}BM}$ blend films annealed at different temperatures with 3 vol% DIO added, (c) the EQE spectrum of P3HT:$\mathrm{PC_{61}BM}$ BHJ solar cells annealed at different temperatures with 3 vol% DIO added.

In conclusion, we have shown that thermal annealing has a significant effect on the performance of 3 vol% DIO added P3HT:$\mathrm{PC_{61}BM}$ BHJ devices by influencing P3HT crystallization and $\mathrm{PC_{61}BM}$ aggregation. It is also found that V_{oc} is mainly influenced by the interplanar spacing of P3HT lamellar, and J_{sc} and FF have a close relationship with the P3HT crystalline domains with better packing order and $\mathrm{PC_{61}BM}$ aggregation, which are attributed to the charge-carrier transportation. These results collectively suggest that thermal annealing alters the driving force by changing the time scale which is responsible for the structure formation in the DIO added P3HT:$\mathrm{PC_{61}BM}$ blend films and the consequent performance of the BHJ devices.

A portion of this work is based on the data obtained at 1W1A, Beijing Synchrotron Radiation Facility (BSRF). We gratefully acknowledge the scientists at the diffusion x-ray scattering station for their assistance in experiments.

References

[1] Tang C W 1986 *Appl. Phys. Lett.* **48** 183
[2] Yu G and Heeger A J 1995 *J. Appl. Phys.* **78** 4510
[3] Zhang Y, Wang H, Liu Z, Zou B, Duan C Y, Yang T, Zhang X J, Zheng C J and Zhang X H 2013 *Appl. Phys. Lett.* **102** 163906
[4] Wang J, Ueda M and Higashihara T 2014 *J. Polym. Sci. Part A: Polym. Chem.* **52** 1139
[5] Li G, Shrotriya V, Huang J, Yao Y, Moriarty T, Emery K and Yang Y 2005 *Nat. Mater.* **4** 864

[6] Kim Y, Cook S, Tuladhar S M, Choulis S A, Nelson J, Durrant J R, Bradley D D, Giles M, McCulloch I and Ha C S 2006 *Nat. Mater.* **5** 197
[7] Campoy-Quiles M, Ferenczi T, Agostinelli T, Etchegoin P G, Kim Y, Anthopoulos T D, Stavrinou P N, Bradley D D and Nelson J 2008 *Nat. Mater.* **7** 158
[8] Kim J Y, Lee K, Coates N E, Moses D, Nguyen T Q, Dante M and Heeger A J 2007 *Science* **317** 222
[9] Li G L, He L J, Li J, Li X S, Liang S, Gao M M and Yuan H W 2013 *Acta Phys. Sin.* **62** 197202 (in Chinese)
[10] Chen W B, Xu Z X, Li K, Chui Stephen S Y, Roy V A L, Lai P T and Che C M 2012 *Chin. Phys.* B **21** 078401
[11] Deschler F, Riedel D, Ecker B, von Hauff E, Da Como E and MacKenzie R C 2013 *Phys. Chem. Chem. Phys.* **15** 764
[12] Song T, Zhang F, Shen X, Zhang X, Zhu X and Sun B 2009 *Appl. Phys. Lett.* **95** 233502
[13] Salleo A 2007 *Mater. Today* **10** 38
[14] Bertho S, Janssen G, Cleij T J, Conings B, Moons W, Gadisa A, D'Haen J, Goovaerts E, Lutsen L, Manca J and Vanderzande D 2008 *Sol. Energy Mater. Sol. Cells* **92** 753
[15] Verploegen E, Mondal R, Bettinger C J, Sok S, Toney M F and Bao Z 2010 *Adv. Funct. Mater.* **20** 3519
[16] Ma W, Yang C, Gong X, Lee K and Heeger A J 2005 *Adv. Funct. Mater.* **15** 1617
[17] Jo J, Kim S S, Na S I, Yu B K and Kim D Y 2009 *Adv. Funct. Mater.* **19** 866
[18] Miller S, Fanchini G, Lin Y Y, Li C, Chen C W, Su W F and Chhowalla M 2008 *J. Mater. Chem.* **18** 306
[19] Li G, Yao Y, Yang H, Shrotriya V, Yang G and Yang Y 2007 *Adv. Funct. Mater.* **17** 1636
[20] Pivrikas A, Neugebauer H and Sariciftci N S 2011 *Sol. Energy* **85** 1226
[21] Salim T, Wong L H, Bräuer B, Kukreja R, Foo Y L, Bao Z and Lam Y M 2011 *J. Mater. Chem.* **21** 242
[22] Lee J K, Ma W L, Brabec C J, Yuen J, Moon J S, Kim J Y, Lee K, Bazan G C and Heeger A J 2008 *J. Am. Chem. Soc.* **130** 3619
[23] De Sio A, Madena T, Huber R, Parisi J, Neyshtadt S, Deschler F, Da Como E, Esposito S and Von Hauff E 2011 *Sol. Energy Mater. Sol. Cells* **95** 3536
[24] Yang S P, Wang T N, Shi J B, Zhang Y, Li X W and Fu G S 2013 *Chin. Phys. Lett.* **30** 108401
[25] Vandewal K, Gadisa A, Oosterbaan W D, Bertho S, Banishoeib F, Van Severen I, Lutsen L, Cleij T J, Vanderzande D and Manca J V 2008 *Adv. Funct. Mater.* **18** 2064
[26] Hallermann M, Da Como E, Feldmann J, Izquierdo M, Filippone S, Martín N, Jüchter S and Von Hauff E 2010 *Appl. Phys. Lett.* **97** 023301
[27] Chabinyc M L 2008 *Polym. Rev.* **48** 463
[28] Rivnay J, Mannsfeld S C B, Miller C E, Salleo A and Toney M F 2012 *Chem. Rev.* **112** 5488
[29] Müller B P 2014 *Adv. Mater.* **26** 7692
[30] Kayunkid N, Uttiya S and Brinkmann M 2010 *Macromolecules* **43** 4961
[31] Wu T M, Blackwell J and Chvalun S N 1995 *Macromolecules* **28** 7349
[32] Treat N D, Brady M A, Smith G, Toney M F, Kramer E J, Hawker C J and Chabinyc M L 2011 *Adv. Energy Mater.* **1** 82
[33] Chen H Y, Yang H, Yang G, Sista S, Zadoyan R, Li G and Yang Y 2009 *J. Phys. Chem.* C **113** 7946
[34] Brown P, Thomas D, Köhler A, Wilson J, Kim J S, Ramsdale C, Sirringhaus H and Friend R 2003 *Phys. Rev.* B **67** 195414
[35] Ecker B, Nolasco J C, Pallarés J, Marsal L F, Posdorfer J, Parisi J and von Hauff E 2011 *Adv. Funct. Mater.* **21** 2705
[36] Xu B and Holdcroft S 1993 *Macromolecules* **26** 4457
[37] Zhokhavets U, Erb T, Hoppe H, Gobsch G and Serdar Sariciftci N 2006 *Thin Solid Films* **496** 679
[38] Jamieson F C, Domingo E B, McCarthy-Ward T, Heeney M, Stingelin N and Durrant J R 2012 *Chem. Sci.* **3** 485
[39] Sun B, Zou G, Shen X and Zhang X 2009 *Appl. Phys. Lett.* **94** 233504
[40] Deschler F, De Sio A, Von Hauff E, Kutka P, Sauermann T, Egelhaaf H J, Hauch J and Da Como E 2012 *Adv. Funct. Mater.* **22** 1461